Majumdar *et al.*
Bulletin of the National Research Centre (2023) 47:142
https://doi.org/10.1186/s42269-023-01117-7

Bulletin of the National Research Centre

RESEARCH

Open Access

Fabrication, design, and in vivo investigation of mesoporous silica-based docetaxel trihydrate nanoparticles for colonic drug delivery

Subhabrota Majumdar[1], Mohini Mondal[1], Anirbandeep Bose[2], Ayan Kumar Kar[1] and Rana Mazumder[3*]

Abstract

Background Mesoporous silica-loaded docetaxel trihydrate nanoparticles are the potential to target drug delivery toward a specific region with high stability and predictable release at the target region. They have large surface areas and mesoporous structures with large pore volumes, leading to high bioavailability and therapeutic efficacy at the disease site. This study demonstrates how nanoparticles can be prepared using an emulsion technique.

Results The ratios of eudragit S100 to eudragit L100 polymers, along with phosphatidylcholine, were varied according to the response surface methodology. Differential scanning colorimetry and fluorinated transmitted infrared spectroscopy studies showed that mesoporous silica particles were successful. All formulations had average particle sizes ranging from 70.65 to 143.01 nm, with a range of zeta potential from 17.6 ± 026 to 21 ± 011. In vitro drug delivery studies were achieved for all formulations with a zeta potential of 17.6 ± 026 to 21 ± 011. As per the statistical optimization by RSM that response model for percentage drug loading (Y_1) was found to be 0.0002 which is p-value < 0.05. Hence, the model is significance. Accordingly percentage drug release at 6 h. (Y_2) p-value was found to be 0.0001 and percentage drug release at 10 h (Y_3) p-value was found to be 0.0002, respectively. So all the models are significant. After oral administration of the docetaxel, plasma levels were measured in vivo bioavailability testing of docetaxel. Docetaxel nanosuspension had a significantly higher C_{max} amount than docetaxel microsuspension (98.03 ± 23.40 ng/ml and 213.67 ± 72.21 ng/ml, respectively, with t_{max} 45 min). Docetaxel was more bioavailable in nanosuspension formulations, according to a bioavailability test of rats.

Conclusion The results suggested that the mesoporous silica could be a great potential nanocarrier in colonic delivery with optimal drug content and controlled release docetaxel trihydrate.

Keywords Mesoporous silica-based nanoparticles, Docetaxel trihydrate, Response surface methodology, Evaluation parameters, In-vivo bioavailability study

Background

Mesoporous silica nanoparticles have been intensively investigated to target the drug delivery toward a specific region with high stability, controlled, and predictable release at the target region due to their honeycombs like mesoporous structure, large pore volume, porous structure, the high surface area, which leads to a high absorption rate, and enhanced bioavailability, suitable for poorly soluble drug and proteins and peptides (Sabio et al. 2019; Sargazi et al. 2022). Recently, mesoporous silica has been getting much more attention from researchers due to its

*Correspondence:
Rana Mazumder
ranapharma.mazumder@gmail.com
[1] Calcutta Institute of Pharmaceutical Technology & Allied Health Sciences, Banitabla, Uluberia, Howrah, West Bengal, India
[2] TAAB Biostudy Services, 69-Ibrahimpur Road, Jadavpur, Kolkata, West Bengal, India
[3] Gitanjali College of Pharmacy, Birbhum, West Bengal, India

low toxicity with high therapeutic efficacy and successful accumulation toward diseases site (Manzano et al. 2018; Samanta et al. 2019).

Targeting drug delivery in the colonic environment to treat colonic disease has proven difficult. Colon-targeted drug delivery refers to drugs that must be released at the target site to demonstrate therapeutic efficacy. There are fewer side effects and no premature drug release. The advantages of colon-targeted drug distribution systems over traditional drug delivery systems include the lower dosage of the drug that is sufficient to produce therapeutic efficacy in the targeted region, a reduced dosing frequency, and fewer systemic adverse effects (Mazumder et al. 2020; Naeem et al. 2020). Many novel advancement technologies, such as carbon nanotubes, quantum dots, mesoporous silica drug delivery systems, and polymeric micelles, can enhance stability, accumulate drugs to the target area to show high therapeutic efficacy, and increase bioavailability (Muthukrishnan et al. 2022; Hossen et al. 2019).

Docetaxel trihydrate, a semisynthetic derivative of taxanes (Fig. 1), effectively treats breast, lung, and pancreatic cancer. As a first-line treatment, this drug is combined with cisplatin (Rarokar et al. 2017). Docetaxel trihydrate is highly hydrophobic, resulting in low systemic absorptivity and low bioavailability, leading to high toxicity, hypersensitivity, musculoskeletal toxicity, and neurotoxicity. Nanoparticulate technology can overcome adverse reactions and adverse events in docetaxel trihydrate.

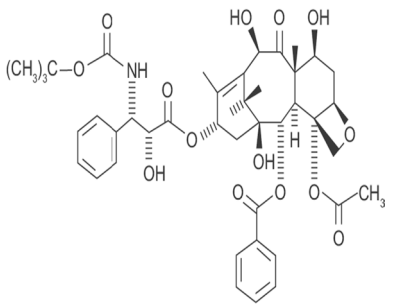

Fig. 1 Chemical structure of docetaxel trihydrate

This study uses pH-dependent polymers to describe the design and evaluation of mesoporous silica particles entrapped with bioactive molecules docetaxel trihydrate. It targets the colonic environment to ensure maximum therapeutic efficacy toward the disease site. The statistical optimization of the mesoporous silica loaded with docetaxel trihydrate nanoparticles was done. All formulations of mesoporous silica-entrapped docetaxel trihydrate nanoparticles were evaluated.

Methods

Materials

Docetaxel trihydrate was gifted from Fresenius Kabi Oncology Ltd, Kalyani, India. Phosphatidylcholine and *Soya lecithin* were purchased from Hi Media. Eudragit S100 and eudragit L100 were purchased from Evonik Rochm Pharma Ltd. Others all chemicals and reagents used in the experiments were of analytical grade, followed by pharmaceutical standards.

Methods

Fabrication of mesoporous silica-loaded docetaxel trihydrate nanoparticles

Docetaxel trihydrate nanoparticles containing mesoporous silica were prepared using oil-in-water emulsion techniques with minor modifications (Choi et al. 2015; Wang et al. 2020). Table 1 lists the ingredients of various nanoparticle formulations. To chloroform containing docetaxel trihydrate, eudragit S100, or eudragit

Table 1 3^2 factorial design with the experimental response values for the various formulation of pH-dependent mesoporous silica-loaded docetaxel trihydrate nanoparticles

Formulation code	Factors (levels)		Responses		
	Ratio of eudragit S100 and L100 (mg) (A)	Phosphatidylcholine (mg) (B)	Entrapment efficiency (%)	Drug release at 6 h (%)	Drug release at 10 h (%)
F1	200 (+1)	60 (0)	78.38	34.31	73.39
F2	200 (+1)	40 (−1)	76.6	32.09	71.45
F3	100 (0)	60 (0)	64.77	24.24	57.16
F4	100 (0)	80 (+1)	59.6	20.03	53.38
F5	40 (−1)	40 (−1)	55.22	18.26	49.28
F6	100 (0)	40 (−1)	69.66	26.89	64.74
F7	200 (+1)	80 (+1)	75.44	31.87	68.48
F8	40 (−1)	80 (+1)	44.83	12.39	38.74
F9	40 (−1)	60 (0)	52.88	15.16	47.03

L100 polymers, an organic phase is created by measuring phosphatidylcholine. An organic phase contained approximately 40 mg of lecithin. The organic phase was added to an aqueous phase that contained 10 ml deionized water and 2 mg mesoporous silicon nanoparticles. After the solution had been heated to 65 °C, it was stirred until it formed a milky phase. 1% v/v tween 20 was then added drop wise to make it opaque. It was then cooled to room temperature. Ultra-centrifugation was used to separate DTV-LNS from docetaxel at 8000 rpm. The centrifugal filter unit was used to reduce the temperature to 4 °C.

Characterization of mesoporous loaded docetaxel trihydrate nanoparticles

FTIR sand DSC studies The interaction between drug and polymers of mesoporous silica-loaded docetaxel trihydrate nanoparticles was determined by using FTIR technique (Nicolet 380). The IR absorption peak of docetaxel trihydrate was taken in the range of 4000 cm^{-1} to 400 cm^{-1} using the KBr disk method. The major peak was reported for the evaluation of purity (Majumdar et al. 2020; Kar et al. 2020).

DSC (Mettler star SW 1550) is used to characterize samples. The temperature range is 25–30 °C, with a heating rate of 10 °C per minute. Samples have an average weight of 2–4 mg. The glass transition temperature and interactions between the drug and excipient are also characterized. The can is used as a reference to accurately weigh the samples into aluminum pans. DSC can also be recorded under liquid nitrogen at 5 °C. Software (Mazumder et al. 2013) was used to calculate the enthalpies.

Particles size determination Photon correlation spectroscopy was employed for measuring the particle size polydispersity (PDI) of docetaxel trihydrate-loaded nanoparticles. The temperature was 25 °C below the fixed angles of 90° in disposable polystyrene curettes. The particle size polydispersity values were examined at the wavelength of 633 nm (Orlowski et al. 2018).

Scanning electron microscopy Scanning electron microscopy helps to determine the uniformity of particle shape and size. Nanoemulsion was raised on the clear glass stub and sodium aurothiomalate was used for the gold coating to visualize under a SEM at the magnification of 10,000 X (Thambiraj et al. 2019).

Encapsulation efficiency The encapsulation efficiency of various formulations of mesoporous silica-loaded docetaxel trihydrate nanoparticles was examined by measuring the free drug concentration in the dispersion medium. 3 ml of prepared nanoparticle dispersion was taken into the centrifuge tube and subjected to centrifuging at 16,000 rpm for 30 min. After centrifugation, the supernatant layer of nanoparticle dispersion was subjected to filtering through Whatman filter paper. After washing and dilution of the supernatant layer of nanoparticles, dispersion was determined through UV–visible spectrophotometer (1700, Shimadzu, Japan) at the wavelength of 229 nm. The drug loading efficiency of prepared nanoparticles was determined by the below-mentioned equation (Azizi-lalabadi et al. 2019; Murugan et al. 2021).

$$\text{Encapsulation efficiency (\%)} = \frac{\text{Amount of drug use} - \text{Amount of untrapped drug} \times 100}{\text{Amount of drug use in formulation}}$$

Zeta potential The zeta potential of the different formulations containing mesoporous silica-loaded docetaxel nanoparticles was determined by using nano ZS90 Zetasizer and the measurement of effective electric charge on nanoparticles size was examined at 25 °C with a fixed angle set to 173° to the reduction of multiple scattering (Verma et al. 2017; Shelake et al. 2018).

In vitro release profile In vitro evaluation of mesoporous silica-loaded docetaxel nanoparticles formulations was done using a dialysis kit (Hi Media, Mumbai, India) and prepared formulation equivalent to 10 ml was placed into a dialysis bag filled with 100 ml pH 6.8 (indicative stomach acid pH) and pH 1.2, with 37 °C. At 50 rpm, the release medium was stirred. The release medium was blended at a rate of 50 rpm. Samples (1 ml) were reserved at predetermined intervals. A new buffer solution of one ml was added to maintain the sink condition. The mesoporous silica-loaded docetaxel trihydrate nanoparticles were measured using a UV spectrophotometer at 229 nm. The cumulative percentage of drug released was estimated based on the pre-generated calibration curve. Each formulation was tested in triplicate (Orlowski et al. 2018; Poltavets et al. 2019).

Release kinetic To evaluate the mechanism of silica-loaded, mesoporous docetaxel trihydrate, nanoparticles of docetaxel trihydrate were released from different formulations. To establish the mechanism of drug releases

from nanoemulsions, the release exponent (n) was calculated using the Korsmeyer–Peppas model.

Experimental design The mesoporous docetaxel trihydrate nanoparticle was statistically optimized using 3^2 models based on factorial designs. The proportion of polymers such as eudragit S100 as well as eudragit L100 (A), and phosphatidylcholine (B) were evaluated as two independent factors and were classified into three levels, including low (−1), medium (0) as well as the highest (+1). The test batch was analyzed by utilizing independent variables at various levels that are suitable to optimize the statistical process of mesoporous silica-loaded pH-dependent docetaxel trihydrate nanoparticles. Three different response or dependent variables include the percentage of efficiency in loading of drugs ($Y1$) and the percentage of the release of medicines after 6 h ($Y2$), and the percentage of drug loading after 10 h ($Y3$). The design and evaluation of the experimental data were performed using StatEase Design Expert 11 trial version, shown in Table 1. The mesoporous silica-loaded docetaxel trihydrate nanoparticles were evaluated on the optimization of dependent variables on independent variables using an equation of polynomial as follows:

$$Y = b_0 + b_1A + b_2B + b_3AB + b_4A^2 + b_5B^2$$

In this research, the variable Y is assumed to be the response variable. b_0 is considered the intercept as well as b_1, b_2, b_3, b_4, and b_5 are regarded as the coefficients of regression, while A and B are the response variables in the equation AB considered to be an interaction between two variables. The validity of the model and all individual parameters of the response can be determined using an ANOVA one-way model. The percent effectiveness of loading drugs of drug loading efficiency, the percent of the release of the drug at 6 h, and the percent of the release of drugs at 10 h are observed. The data are used to determine the targets specified as the independent variables (Sun et al. 2018).

Statistical analysis The statistical optimizations of nanoparticles were calculated using design expert software. The statistical analysis was achieved by ANOVA analysis. The p value was examined as statistically significant.

Accelerated stability study

The accelerated stability test of optimized formulations should be used to forecast the stability study by international conference on harmonization (ICH) guidelines with little abatement. The optimized formulation should be placed in ambient color vials and sealed with aluminum foil to allow for the short-term, accelerated stability test at 40 ± 5% relative humidity (RH) and 75 ± 5% relative humidity (RH). The sample was tested over three months. At various intervals, the sample was collected and examined to determine stability. The parameters included physical appearance clarity, clarity, pH, and entrapment efficiency (Mazumder et al. 2021).

In vivo bioavailability study

This study examined the pharmacokinetics of a nanosuspension of docetaxel trihydrate. It was used for measuring docetaxel plasma levels following oral administration. This was done in an experiment that involved a two-way crossover design. Here, six healthy male rats were used (200–250 g). It was accomplished by animal ethical standards (Tazeze et al. 2021). As a test sample, the rats received docetaxel nanosuspension each session and the pure drug docetaxel at a specific time. The pure drug and formulation were administered orally to each animal at 1.5 mg/kg using an oral feeding tube.

Pharmacokinetics For the study, we used the HPLC (Shimadzu Corp. HPLC). The mobile phase was made using a 30:70 phosphate buffer and methanol at a 1 ml/min flow rate. The retro-orbital puncture technique collected 0.5 ml of blood before dosing (0 h) and at 0, 0.5, 1, and 2 h. Samples were centrifuged for 10 min at 5500 rpm. Blood plasma was preserved and collected at 20 °C (Mazumder et al. 2022). Mix 0.1 ml of blood with 0.5 ml of acetonitrile to extract the drug and let it sit for 10 min. Transfer 150 µl plasma and 50 mg IS into 1.5 ml centrifuge tubes. Deproteinization is completed after adding 300 ml of acetonitrile, shaking each sample for five minutes, and centrifuging the samples at 6600 rpm for five minutes. Micropipettes were used to collect the supernatant solutions of each sample. The filtrate was then passed through a filter of 0.45 micron (μ). The HPLC was used to introduce 20 micro liters of the top pure layer.

Pharmacokinetics analysis The pharmacokinetic studies were done by the plot between drug concentration and time to determine the pharmacokinetic parameters, such as C_{max}, t_{max}, $AUC_{0\text{-}t}$, $AUC_{0\text{-inf}}$, $t_{1/2}$, and K_{el} (Ghelicha et al. 2019). Various pharmacokinetics constraints estimated the relative bioavailability of docetaxel, and statistical studies were presented by the mean ± SD using SPSS 13 software.

Results

Fabrication of mesoporous silica-loaded docetaxel trihydrate nanoparticles

Mesoporous silica-loaded docetaxel trihydrate nanoparticles were formulated by emulsion technique with negligible moderation employing the polymer ratio of eudragit L100 and eudragit S100 using response surface method (Table 1) (Luna et al. 2021; Narayan et al. 2018). Docetaxel trihydrate used as model drug. The nanoparticles were prepared with organic phase containing phosphatidylcholine added to chloroform dispersed to aqueous phase containing 10 ml of deionized warm water and 2 mg mesoporous silica nanoparticles. The preparations were heated at 65 °C with continuous stirring. In this study, all nanoemulsions contained tween 20, an emulsifying agent for the preparation of stable form added drop wise and cooled down at room temperature.

Characterization of mesoporous loaded docetaxel trihydrate nanoparticles

FTIR sand DSC studies

The FTIR spectrum of docetaxel trihydrate, eudragit S100, and eudragit L100 is shown in Fig. 2. Docetaxel trihydrate has a melting point in the range of 114.52 °C. The thermogram peak of the drug (docetaxel trihydrate) and polymers (eudragit S100 and L100) is described in Fig. 3 (Joshi et al. 2019).

Particles size determination and polydispersity index (PDI)

The particle size of different formulations containing eudragit-loaded mesoporous silica-loaded docetaxel trihydrate nanoparticles is mentioned in Table 2. Particle sizes of mesoporous silica-loaded docetaxel trihydrate nanoparticles were observed in between the range of 72.81 nm to 110.97 nm (Ibrahim et al. 2020).

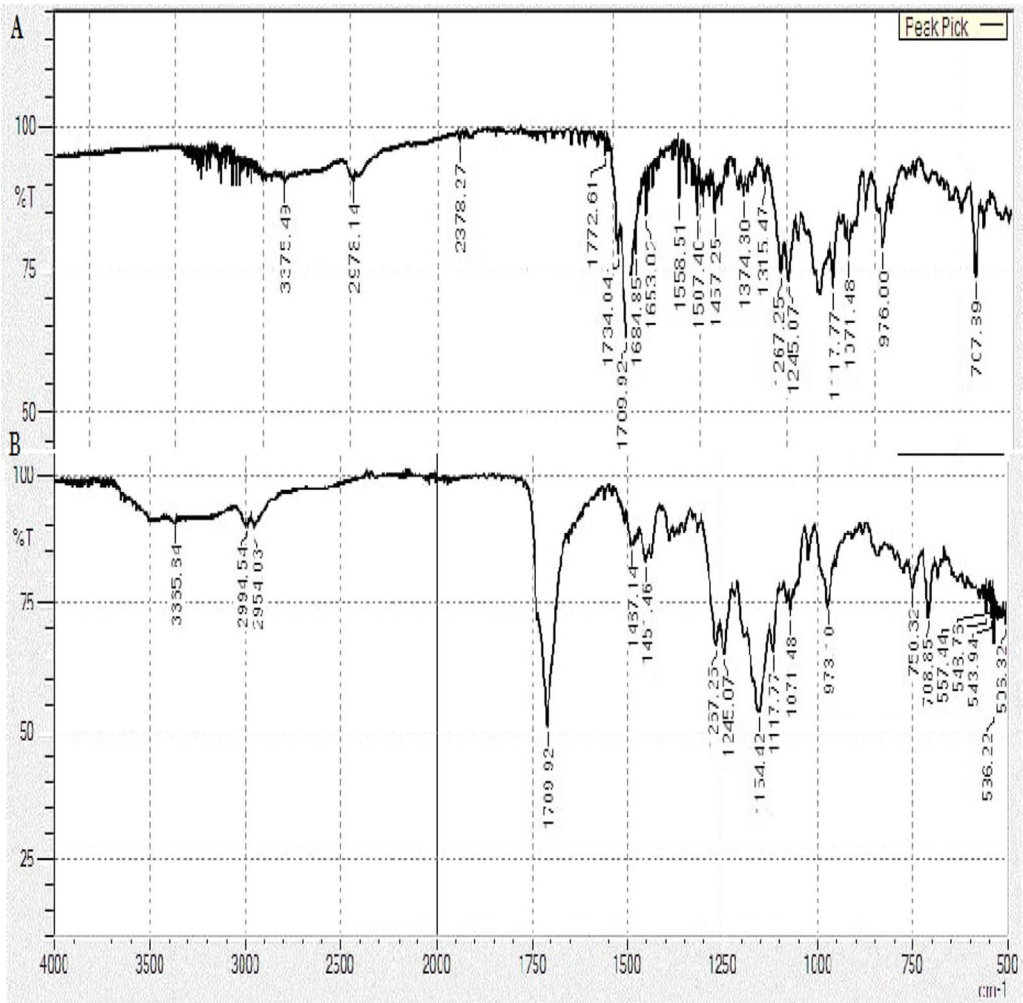

Fig. 2 FTIR Data of the final formulation: **A** docetaxel trihydrate model drug and **B** model drug with excipients

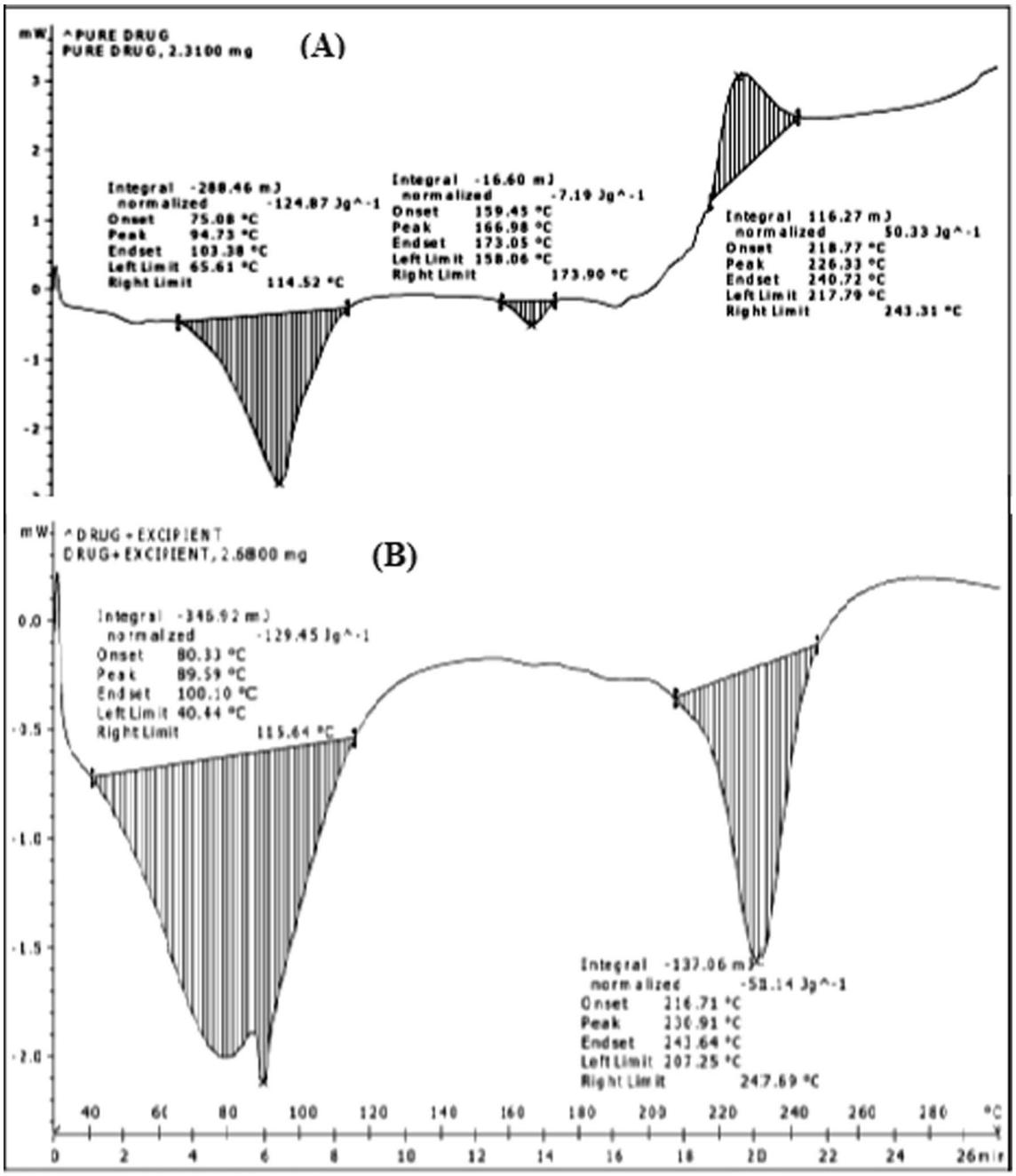

Fig. 3 Differential scanning colorimetry (DSC) study of **A** docetaxel trihydrate and **B** docetaxel trihydrate with excipients

Scanning electron microscopy (SEM)

The single emulsion preparation process was successful in producing mesoporous silica-loaded docetaxel trihydrate nanoparticles employing tween 20 as the surfactant in the formulation and analysis of the SEM image demonstrated the morphological characteristics of the nanoparticles and shown in Fig. 4 (Pandita et al. 2021).

Encapsulation efficiency

Various formulations of drug entrapment efficiency of mesoporous silica-loaded docetaxel trihydrate nanoparticles were observed within the range of 44.83 ± 0.5% to 78.38 ± 0.25% (Kassem et al. 2019).

Table 2 Zeta potential and particle size of different formulations (mean ± S.D; $n = 3$)

Formulation code	Zeta potential (mv)	Particle size (nm)	Polydispersity index (PI)
F1	− 21.1 ± 0.11	73.08 ± 1	0.191
F2	− 19.3 ± 0.23	72.81 ± 1.2	0.257
F3	− 18.9 ± 0.25	84.51 ± 1	0.191
F4	− 18.7 ± 0.23	92.88 ± 3	0.257
F5	− 18.6 ± 0.01	86.31 ± 2	0.191
F6	− 18.4 ± 0.12	83.61 ± 2	0.257
F7	− 18.0 ± 0.14	104.85 ± 1.5	0.191
F8	− 17.8 ± 0.24	110.97 ± 1	0.257
F9	− 17.6 ± 026	101.52 ± 2	0.191

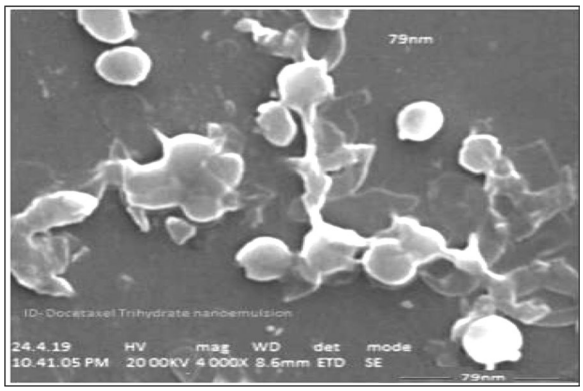

Fig. 4 Mesoporous silica-loaded docetaxel trihydrate nanoemulsion under scanning electron microscope (SEM)

Zeta potential

Zeta potential values of various formulations containing mesoporous silica-loaded docetaxel trihydrate nanoparticles are mentioned in Table 2. The zeta potential of mesoporous loaded docetaxel trihydrate nanoparticles was observed within the range of − 18.0 ± 0.14 mv to − 21.1 ± 0.11 mv, considering that prepared nanoparticles had enough charge at their surface which prohibits exhibition due to repulsion of electric charges (Sawyer 2009).

In vitro release profile

The in vitro dissolution summary (Peng et al. 2020) of different formulations containing mesoporous silica-loaded docetaxel trihydrate nanoparticles is mentioned in Fig. 5. Through the data analysis, the *F*1 formulation containing 60 mg of phosphatidylcholine and a 1:0 ratio of eudragit S100 and L100 was released at 73.39% at 10 h.

Release kinetic

The in vitro dissolution data of mesoporous silica-loaded docetaxel trihydrate formulation were suitable for various kinetic equations and the correlation coefficient (R^2) value was calculated from different kinetics models and through correlation coefficient (R^2) value the release mechanism was calculated in Table 3.

Formulation optimization by experimental design and statistical analysis

The mesoporous silica-loaded docetaxel trihydrate was optimized by 3^2 full-factorial designs (Table 1). In this full-factorial design, the ratio of eudragit polymers (S100 and

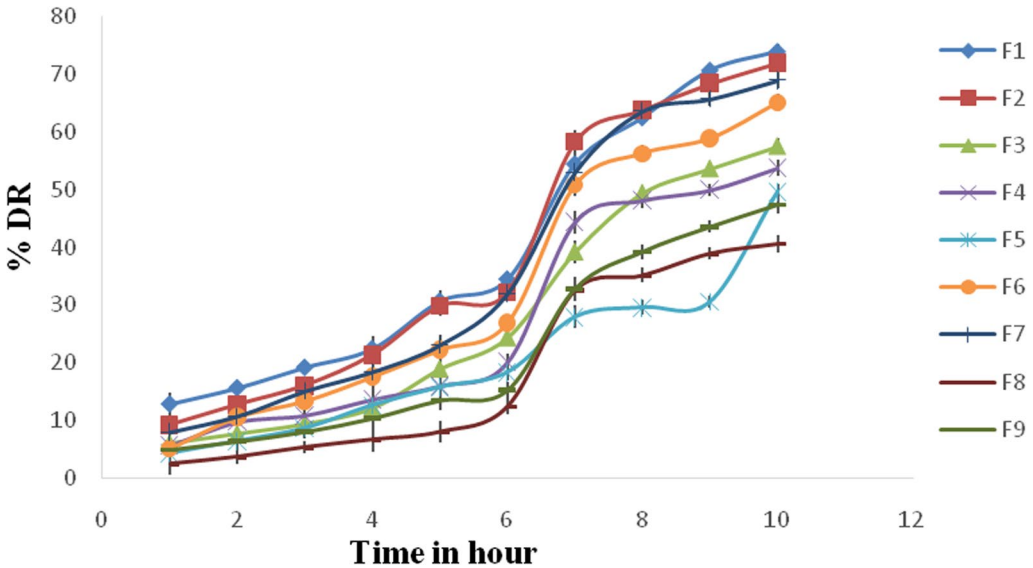

Fig. 5 In vitro release profile of mesoporous silica-loaded docetaxel trihydrate nanoparticle (mean ± S.D, $n = 3$)

Table 3 Different release kinetic of mesoporous silica nanoparticles

Formulation	Zero order		First order		Higuchi mechanism		Korsmeyer–Peppas	
	R^2	*n*	R^2	*n*	R^2	*n*	R^2	*n*
*F*1	0.949	7.586	0.909	−0.063	0.884	31.28	0.941	1.135
*F*2	0.944	7.914	0.913	−0.062	0.890	32.85	0.957	1.324
*F*3	0.940	6.540	0.921	−0.042	0.867	26.71	0.938	1.494
*F*4	0.898	6.041	0.880	−0.038	0.834	24.88	0.921	1.401
*F*5	0.908	4.423	0.854	−0.026	0.839	18.17	0.974	1.380
*F*6	0.940	7.259	0.911	−0.051	0.884	30.09	0.971	1.522
*F*7	0.936	7.813	0.908	−0.059	0.876	32.31	0.952	1.394
*F*8	0.881	4.986	0.856	−0.027	0.806	20.38	0.998	1.836
*F*9	0.909	5.267	0.896	−0.030	0.830	21.51	0.918	1.467

L100) and phosphatidylcholine were used as dependent variables based on various trial batches responses and varied at three different levels low (−1), medium (0), and high (+1). The three different response variables such as the percentage (%) of drug loading efficiency, percentage (%) of drug release at 6 h, and percentage (%) of drug release at 10 h are observed. The different investigated response is denoted using a quadratic equation as follows:

$$\text{Entrapment efficiency (\%)} = 63.2733 + 235{,}333A + 1.89B + 6.43AB + 0.8A^2 + 0.52B^2$$

where F value = 85.45, $R^2 = 0.998$, $p < 0.05$.

$$\text{Drug release at 6 h(\%)} = 22.7111 + 1.38333A + 2.04667B + 1.12333A^2 + 0.68333B^2$$

where F value = 113.47, $R^2 = 0.982$, $p < 0.05$.

Table 4 Summary of ANOVA for response surface quadratic models

Source	Sum of square	Degree of freedom	Mean square	*F*-value	*P*-value prob > *F*
Entrapment efficiency (%)					
Model	1048.28	2	524.14	46.15	0.0002
A	970.45	1	970.45	85.45	< 0.0001
B	77.83	1	77.83	6.85	0.0397
AB	165.38	1	165.38	0.5546	0.0510
A^2	1.28	6	11.36	0.0043	0.0951
B^2	0.5408	1	0.5408	0.0018	0.0968
Drug release at 6 h (%)					
Model	479.78	2	239.89	60.24	0.0001
A	451.83	1	451.83	113.47	< 0.0001
B	27.95	1	27.95	7.02	0.0381
AB	1021.44	1	70.81	0.5408	0.0515
A^2	2.52	1	2.52	0.0193	0.0898
B^2	0.9339	1	0.9339	0.0071	0.9380
Drug release at 10 h (%)					
Model	1097.12	2	548.56	52.08	0.0002
A	993.20	1	993.20	94.29	< 0.0001
B	103.92	1	103.92	9.87	0.0200
AB	122.77	1	122.77	0.3766	0.05828
A^2	0.2813	1	0.2813	0.0009	0.9784
B^2	0.0968	1	0.0968	0.0003	0.9873

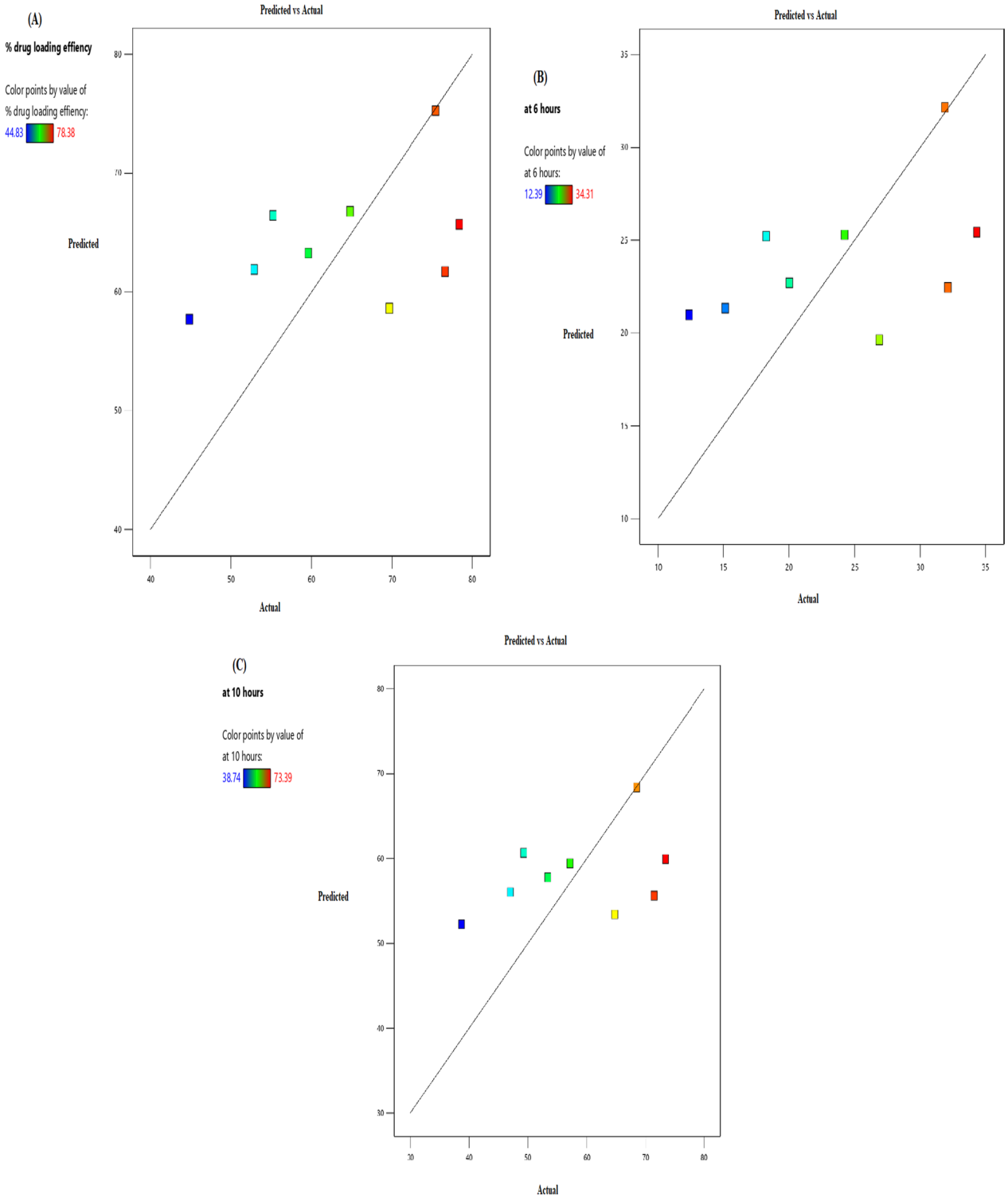

Fig. 6 Linear correlation plot of **A** percentage (%) drug loading efficiency **B** percentage (%) drug release at 6 h **C** percentage (%) drug release at 10 h between actual value and predicted value

$$\text{Drug release at 10 h (\%)} = 57.7867 + 2.525A + 1.94667B + 5.54AB + 0.375A^2 + 0.22B^2$$

where F value = 94.29, $R^2 = 0.998$, $p < 0.05$.

From the above-mentioned equation, the high value of the correlation coefficient signifies that the investigated responses are associated strongly with the factors studied during the experiment. The ANOVA results are shown in Table 4. The model simplification of the

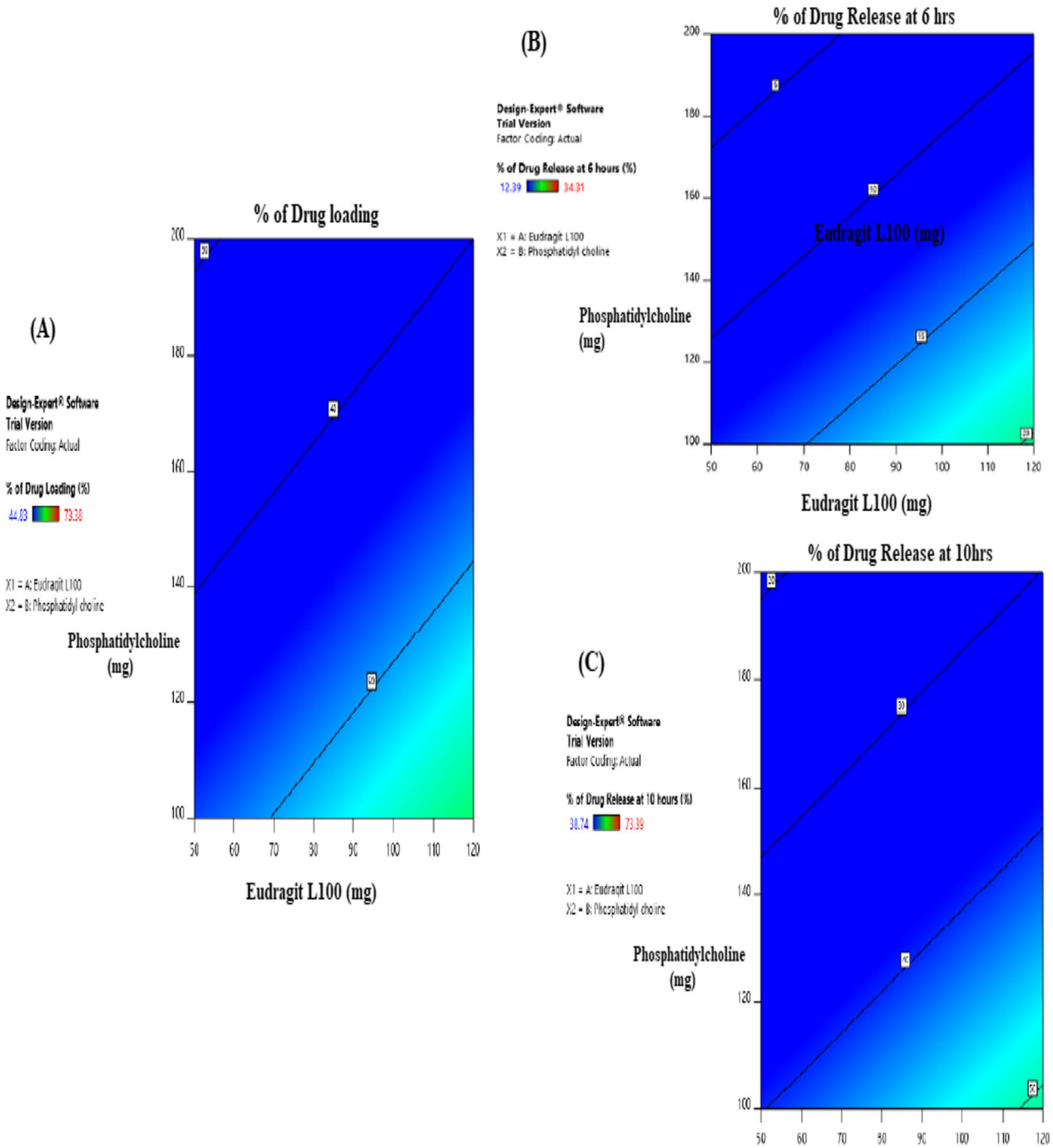

Fig. 7 Contour plot observing the effect of ratio of **A** eudragit [× 1] and phosphatidylcholine on percentage (%) of drug loading on the formulation, **B** eudragit [× 1] and phosphatidylcholine on percentage (%) of drug Release at 6 h on the formulation and **C** eudragit [× 1] and phosphatidyl choline on percentage (%) of drug release at 10 h on the formulation

quadratic above-mentioned equation was considered for eliminating the nonsignificant ($p > 0.05$) terms.

The linear correlation plots of actual and predictable results with the corresponding residual plot of entrapment efficiency (%), drug release at 6 h (%), and drug release at 10 h (%) are presented in Figs. 1, 2, 3, and corresponding residual plots show a scatter between residual versus predictable value of entrapment efficiency (%), drug release at 6 h (%), and drug release at 10 h (%) presented in Fig. 6.

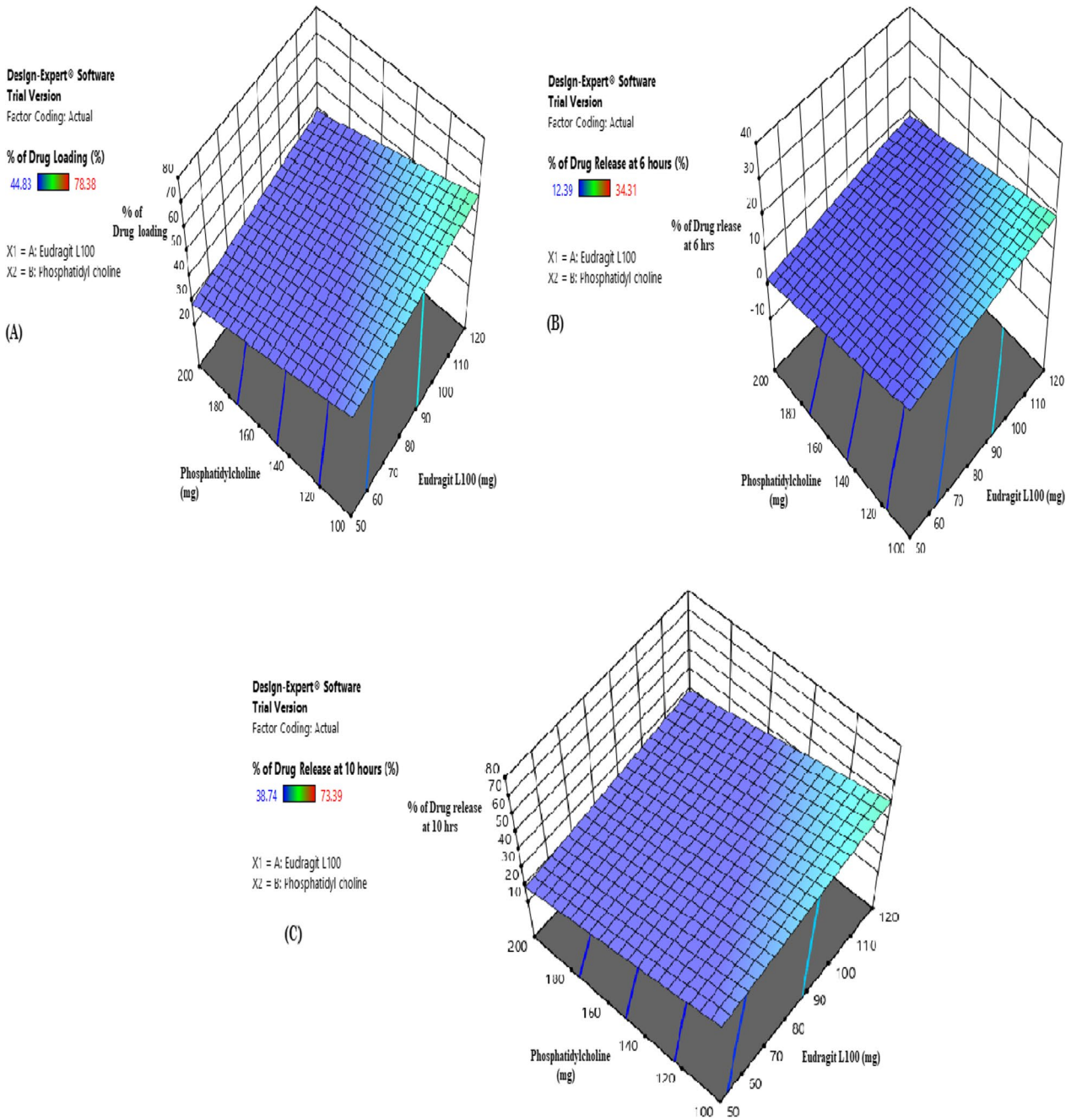

Fig. 8 Response surface plot observing the effect of ratio of **A** eudragit [x_1] and phosphatidylcholine [x_2] on percentage (%) of drug loading on the formulation, **B** eudragit [x_1] and phosphatidylcholine on [x_2] percentage (%) of drug release at 6 h on the formulation and **C** eudragit [x_1] and phosphatidyl choline on [x_2] percentage (%) of drug release at 10 h on the formulation

Ratio of eudragit S100, L100, and phosphatidylcholine as the independent variables impacts on response variables such as entrapment efficiency (%), drug release at 6 h (%), and drug release at 10 h (%) were explicated using three-dimensional response surface plot and two-dimensional contour plot [40] which related with entrapment efficiency (%) (Fig. 7). The response surface design also confirms that the linear curve of the ratio of eudragit s100 and L100 was almost flattered and was seen for the phosphatidylcholine (Fig. 8).

The contour plot (Fig. 7) of drug release at 6 h (%) factors *A* (ratio of eudragit S100 and L100) and *B* (phosphatidylcholine) showed that linearity increased of drug release at 6 h (%) with an increase in the ratio of eudragit s100 and L100 (*A*) and phosphatidylcholine (*B*) at the low level of (− 1) of phosphatidylcholine (*B*) the drug release was increased ($p < 0.05$) significantly when *A* increase from − 1 level to + 1 level. The response surface design (Fig. 7) also relating to the drug release at 6 h (%) designated that linear curvature on the ratio of eudragit S100 and eudragit L100 (*A*) and phosphatidylcholine (*B*) and considered as both *A* and *B* impacts release rate at 6 h (%).

The contour plot (Fig. 7) of drug release at 10 h versus independent factors involved in such ratio of eudragit S100 and L100 (*A*) and phosphatidylcholine (*B*) that the linearity increases drug release with both independent variables. In another way, a nonlinear curve slightly increases the percentage of drug release at 10 h and was identified with an increase in the ratio of eudragit S100 and eudragit L100 (*A*). The drug release was significantly increased ($p < 0.05$) when *B* increased from the low level (− 1 to + 1) of *A* (Fig. 8).

After the determination of polynomial equations for the independent as well as the dependent variables, to get an optimized formulation with the desired responses the combination was statistically optimized for all three different responses. Trading off various responses, the desired responses were restricted as 44.83% ≥ entrapment efficiency (%); 34.31 ≥ drug release at 6 h, and 73.39 ≤ drug release at 12 h. After all comprehensive evaluation of the responses with adequate observation, the formulation containing 60 mg of phosphatidylcholine and 1:0 ratio of eudragit S100 and L100 was the maximum desired requisites. After examination of all the responses, the *F*1 formulation was considered an optimized formulation.

Table 5 Result of various parameters of optimized formulation at different time intervals under accelerated stability condition

Time period (month)	Visual appearance	Clarity	Entrapment efficiency (%)	pH
0	Yellowish	Cloudy	77.24 ± 0.36	6.4
1	Yellowish	Cloudy	78.11 ± 1.01	6.7
2	Yellowish	Cloudy	76.78 ± 0.62	6.5
3	Yellowish	Cloudy	77.89 ± 1.31	6.8

Accelerated stability study

The pH-dependent polymer-gated mesoporous silica nanoparticles of docetaxel trihydrate nanoemulsion formulation showed a good stability during the period of 3 months (Iyer et al. 2015). The appearance of formulation (Table 5) was yellowish in color and cloudy. The pH was also found to be within the range of 6.4–6.8, which is desirable for colon targeting.

In vivo bioavailability study

Docetaxel was measured in plasma following oral administration using the in vivo bioavailability test of docetaxel. Comparing pure drug microsuspension and docetaxel nanosuspension demonstrated enhanced bioavailability (Table 6 and Fig. 9). A C_{max} of docetaxel following orally administered docetaxel microsuspension was 98.03 ± 23.40 ng/ml and then it took 45 min to reach t_{max} and docetaxel nanosuspension had C_{max}, and the t_{max} was 213.67 ± 72.21 ng/ml and 45 min, respectively. The C_{max} quantity of docetaxel nanosuspension (formulation) compared with docetaxel microsuspension (control) of 98.03 ± 23.40 ng/ml and 213.67 ± 72.21 ng/ml (Jackson et al. 2020). The $AUC_{0\text{-inf}}$ was significantly elevated in docetaxel-based

Table 6 Comparison of pharmacokinetic data of docetaxel nanosuspension (formulation) and pure docetaxel powder (control) as microsuspension

Pharmacokinetic parameters	Pure docetaxel microsuspension (control)		Docetaxel nanosuspension (formulation)	
C_{max} (ng/ml.)	Mean	98.03	Mean	213.67
	± S.D	23.40	± S.D	72.21
t_{max} (min)	Mean	45.00	Mean	45.00
	± S.D	0.00	± S.D	0.00
AUC_{0-t} (ng. min/ml.)	Mean	9627.76	Mean	28,345.41
	± S.D	2298.52	± S.D	9687.11
AUC_{0-inf} (ng. min/ml.)	Mean	9967.14	Mean	31,955.93
	± S.D	2386.35	± S.D	11,145.17
k_{el} (min^{-1})	Mean	0.007	Mean	0.005
	± S.D	0.000	± S.D	0.000
$t_{1/2}$ (min)	Mean	93.18	Mean	133.34
	± S.D	3.47	± S.D	7.61

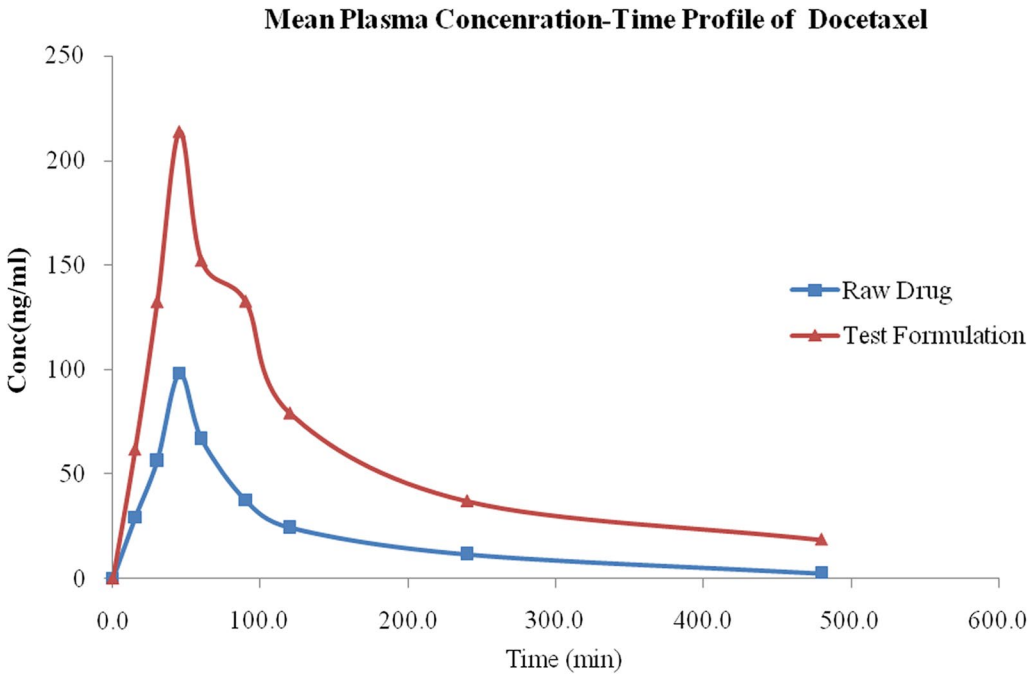

Fig. 9 Plasma concentration–time curves of pure docetaxel microsuspension (control) and docetaxel nanosuspension (formulation)

nanosuspension, compared to microsuspension containing docetaxel ranging from 9967.14 ± 2386.35 in ng/ml up to 31,955.93 ± 11,145.17 ng/ml.

Discussion

The formulations were designed by 3^2 full-factorial designs using eudragit polymers (S100 and L100) and phosphatidylcholine as dependent variables giving relevant results compared to the conventional product.

Several vibrational peaks of docetaxel trihydrate were observed in FTIR. The NH stretching of alkanes, C–O stretching vibration, N–H plane bonding vibrations, and C=O stretching were observed at 3432 cm^{-1}, 1782 cm^{-1}, 1635 cm^{-1}, and 720 cm^{-1}. With the drug and polymers mixture, peaks were observed at 3375 cm^{-1}, 1772.61 cm^{-1}, 1684.85 cm^{-1}, and 707.89 cm^{-1} (Zhuang et al. 2020). The two graphs of stretching vibrational peaks were matched each other, showing that the drug sample used is pure and stable and there are no such interactions were found with drug and polymers. The DSC thermogram peak of the drug and polymers was found in the range of 115.64 °C. The two graphs of the thermogram were matched with each other and conclude that there is no such interaction found between the drug and polymers.

The pH-dependent polymer-gated mesoporous silica-loaded docetaxel trihydrate nanoparticles had a narrow size distribution in addition to a significant difference in the distribution between pH-dependent polymer-gated mesoporous–silica nanoparticles of docetaxel trihydrate and drug-free pH-dependent polymer-gated mesoporous silica-loaded docetaxel trihydrate nanoparticles was observed.

The SEM of nanoparticles is smooth with a uniform spherical shape and it also approved the particle size found in the particle size analysis.

The poor encapsulation efficiency of mesoporous silica-loaded docetaxel nanoparticles is due to low solubility and it has been examined that nanoparticles increased drug encapsulation efficiency and reduced drug leakage as well as prolonged residence and accumulation of drugs at target sites. The drug loading efficiency (%) was enhanced significantly ($p < 0.05$) as the ratio of eudragit S100 and L100 and phosphatidylcholine were increased.

The zeta potential range of the nanoparticles is within the range of ± 30 mv, it shows less coalescence and stable nanoparticles due to electrostatic repulsion between particles. The significance of the zeta potential value indicates the stability of the nanoparticles with less coalescence of formulated mesoporous silica-loaded docetaxel trihydrate nanoparticles.

The in vitro dissolution summary of mesoporous silica-loaded docetaxel trihydrate has significant ($p < 0.05$) enhancement due to the large surface area leading to small particle sizes and polymers (eudragit S100 and L100) as well as surfactant played an important role

in the release rate. This evidence shows that the potential release of mesoporous silica-loaded docetaxel trihydrate indicates the enhancement of therapeutic efficacy through the predictable release of docetaxel trihydrate at the target site. The release pattern of mesoporous silica-loaded docetaxel trihydrate followed zero-order kinetics and also followed the Korsmeyer–Peppas model indicated from the highest R^2 value and n exponent.

The RSM study using design expert software helps to determine individual main factors and interaction factors using the quadratic equation. The ANOVA result clearly states that both the factors such as the ratio of eudragit S100 and L100 and phosphatidylcholine had a significant value ($p < 0.05$) effect on entrapment efficiency (%), drug release at 6 h (%), drug release at 10 h (%). Our results shows that nonlinearity decreased the entrapment efficiency with increase independent variables of phosphatidylcholine and entrapment efficiency linearly increase with the ration of eudragit S100 and L100 increase, where A mainly increases from -1 to $+1$ level. From the response surface plot, entrapment efficiency was more dependent on the ratio of eudragit S100 and L100 (A) compared to phosphatidylcholine. The results of the response surface plot of drug release showed that greater curvature toward the ratio of eudragit s100 and L100 (A) and flattering of the curve toward phosphatidylcholine as both independent variables impact the release rate.

There is no significant change of clarity and physical appearance was observed by the stability study. The centrifuge test also showed that the formulation had good physical stability. The good stability might be due to low particle size and effect of tween 20. No degradation of docetaxel trihydrate in optimized formulation was also observed.

In vivo studies shown, Cmax quantity of docetaxel significantly increased when using nanosuspension (formulation) compared with docetaxel microsuspension and arise in relative bioavailability to the dose was determined to be 3 times. The bioavailability study of rats showed that docetaxel's bioavailability was higher for the nanosuspension formulation.

Conclusions

The mesoporous silica-loaded docetaxel trihydrate nanoparticles were successfully applied to the oil-in-water emulsion and formulation was statistically optimized by 3^2 factorial designs, the investigation was done on independent variables (ratio of eudragit S100 and L100 and phosphatidylcholine) and dependent variables (entrapment efficiency, drug release at 6 h, and drug release at 10 h). Upon all the comprehensive evaluation of formulation, it was found the formulations, $F1$ containing 60 mg of phosphatidylcholine and a 1:0 ratio of eudragit s100 and L100 full filled the maximum desired requisites. The bioavailability of docetaxel trihydrate is very poor. This can be overcome by formulating nanoparticles, which can release the drug in a controlled pattern. The polymer concentration plays a major role in the design of control release of nanoparticles. A higher concentration of phosphatidylcholine provides good control of the release of the drug for an anticipated period. Systematic studies using the design of experiment optimization could surmount the hiccup of balancing coveted drug release patterns using the polymer combination. The choice of experimental design, i.e., central composite design was found to be highly appropriate as it can detect any nonlinearity in factor–response relationship with minimal expenditure of development effort and time. Docetaxel was measured in plasma following oral administration using the in vivo bioavailability test of docetaxel. Comparing pure drug microsuspension and docetaxel nanosuspension demonstrated enhanced bioavailability. The rise in relative bioavailability to the dose was determined to be 3 times. The bioavailability study showed that docetaxel's bioavailability was higher for the nanosuspension formulation. The optimized formulation exposited excellent controlled release characteristics vouching for the success of the experimental approaches followed.

Abbreviations

PDI	Polydispersity index
SEM	Scanning electron microscopy
FTIR	Fourier transform infrared spectroscopy
DSC	Differential scanning colorimeter
RSM	Response surface method
C_{max}	Maximum plasma concentration
t_{max}	Time to attain maximum concentration
K_{el}	Plasma elimination rate constant
HPLC	High-performance liquid chromatography

Acknowledgements

Authors wish to give thanks to Calcutta institute of pharmaceutical technology, Howrah, West Bengal, India, and TAAB biostudy services, 69-Ibrahimpur Road, Jadavpur, Kolkata, West Bengal, India, given research laboratory to carry out this project work and also thanks to Gitanjali college of pharmacy, Birbhum, West Bengal, India, for help in completion of the research project work.

Author contributions

We declare that this work was done by the authors named in this manuscript: SM, MM, AB, and RM conceived and designed the study. MM, AB, and AKK carried out the laboratory work, collected and analyzed the data and RM drafted the manuscript. SM supervised the work and MM assisted in the data analysis. All authors have read and approved the final manuscript.

Funding

The authors have no funding to report.

Availability of data and materials

All necessary data generated or analyzed during this study are included in this manuscript. Any additional data could be available from the corresponding author upon request.

Declarations

Ethics approval and consent to participate
The authors assert that all procedures contributing to this work comply with the ethical standards of the Institutional Animal Ethics Committee "TAAB Biostudy Services," 69-Ibrahimpur Road, Jadavpur, Kolkata–700032, India, and ethical approval number is 1938/PO/Rc/S/17/CPCSEA.

Consent for publication
Not applicable.

Competing interests
The authors declare that they have no competing interests.

Received: 2 June 2023 Accepted: 20 September 2023
Published online: 04 October 2023

References

Azizi-Lalabadi M, Ehsani A, Divband B, Alizadeh-Sani M (2019) Antimicrobial activity of titanium dioxide and Zinc oxide nanoparticles supported in 4A zeolite and evaluation the morphological characteristic. Sci Rep 9(1):1–10

Choi J, Ko E, Chung HK, Lee JH, Ju EJ, Lim HK, Park I, Kim KS, Lee JH, Son WC, Lee JS, Jung J, Jeong SY, Song SY, Choi EK (2015) Nanoparticulated docetaxel exerts enhanced anticancer efficacy and overcomes existing limitations of traditional drugs. Int J Nanomed 10:6121

Ghelicha R, Jahannamab MR, Abdizadeha H, Torknikc FS, Vaezic MR (2019) Central composite design (CCD)-response surface methodology (RSM) of effective electrospinning parameters on PVP-B-Hf hybrid nanofibrous composites for synthesis of HfB2-based composite nanofibers. Compos B 166:527–541

Hossen S, Hossain MK, Basher MK, Mia MNH, Rahman MT, Uddin MJ (2019) Smart nanocarrier-based drug delivery systems for cancer therapy and toxicity studies: a review. J Adv Res 15:1–18

Ibrahim AH, Smått JH, Govardhanam NP, Ibrahim HM, Ismael HR, Afouna MI, Samy AM, Rosenholm JM (2020) Formulation and optimization of drug-loaded mesoporous silica nanoparticle-based tablets to improve the dissolution rate of the poorly water-soluble drug silymarin. Eur J Pharm Sci 142:105103

Iyer V, Cayatte C, Guzman B, Schneider-Ohrum K, Matuszak R, Snell A, Rajani GM, McCarthy MP, Muralidhara B (2015) Impact of formulation and particle size on stability and immunogenicity of oil-in-water emulsion adjuvants. Hum Vaccin Immunother 11(7):1853–1864

Jackson AJ, Conner DP, Miller R (2020) First measured plasma concentration value as C_{max}; impact on the C_{max} confidence interval in bioequivalence studies. Biopharm Drug Dispos 21(4):139–146

Joshi R, Raje S, Akram W, Garud N (2019) Particle engineering of fenofibrate for advanced drug delivery system. Future J Pharm Sci 5:1–11

Kar AK, Shil A, Kar B, Dey S (2020) Formulation development and statistical optimization of zingiberol incorporated sodium alginate-methyl cellulose blend microspheres. Int J Biol Macromol 162:1578–1586

Kassem MA, Shaboury KMEL, Mohamed AI (2019) Application of central composite design for the development and evaluation of chitosan-based colon targeted microspheres and in-vitro characterization. Ind J Pharm Sci 81(2):354–364

Luna RC, Illana AM, Perez FN, Caro RR, Veiga MD (2021) Naturally occurring polyelectrolytes and their use for the development of complex-based mucoadhesive drug delivery systems: an overview. Polymers 13:2241

Lv Y, He H, Qi J, Lu Y, Zhao W, Dong X, Wu W (2018) Visual validation of the measurement of entrapment efficiency of drug nanocarriers. Int J Pharm 547(1–2):395–403

Majumdar S, Dey S, Ganguly D, Mazumder R (2020) Enhanced topical permeability of natural flavonoid baicalein through nano liposomal gel: in-vitro and in-vivo investigation. J Drug Deliv Sci Technol 57:101666

Manzano M, Vallet-Regí M (2018) Mesoporous silica nanoparticles in nanomedicine applications. J Mater Sci Mater Med 29(5):1–14

Mazumder R, Allamneni Y, Firdous SM, Parya H, Chowdhury AD (2013) Formulation, development and in-vitro release effects of ethyl cellulose coated pectin microspheres for colon targeting. Asian J Pharmaceut Clin Res 6(5):138–144

Mazumder R, Mahanti B, Majumdar S, Pal R, Chowdhury AD (2020) Improved comprehensive analytical method for assessment of satranidazole in drug and product. Future J Pharmaceut Sci 6(1):1–11

Mazumder R, Mahanti B, Majumdar S, Pal R, Chowdhury AD (2021) Response surface method for optimization of prepared satranidazole powder layered pellets. Future J Pharmaceut Sci 7:190

Mazumder R, Mahanti B, Majumdar S, Pal R, Pahari N (2022) Satranidazole-loaded chitosan/locust bean gum/xanthan gum polysaccharide composite multiunit pellets for colon targeting: in vitro–in vivo investigation. Beni-Suef Univ J Basic Appl Sci 11:151

Murugan B, Krishnan UM (2021) Differently sized drug-loaded mesoporous silica nanoparticles elicit differential gene expression in MCF-7 cancer cells. Nanomedicine 16(12):1017–1034

Muthukrishnan S, Anand AV, Palanisamy K, Gunasangkaran G, Ravi AK, Balasubramanian B (2022) Novel organic and inorganic nanoparticles as a targeted drug delivery vehicle in cancer treatment. Emerg Nanomater Adv Technol 1:17–61

Naeem M, Awan UA, Subhan F, Cao J, Hlaing SP, Lee J, Im E, Jung Y, Yoo JW (2020) Advances in colon-targeted nano-drug delivery systems: challenges and solutions. Arch Pharm Res 43(1):153–169

Narayan R, Nayak UY, Raichur AM, Garg S (2018) Mesoporous silica nanoparticles: a comprehensive review on synthesis and recent advances. Pharmaceutics 10:118

Orlowski P, Zmigrodzka M, Tomaszewska E, Ranoszek-Soliwoda K, Czupryn M, Antos-Bielska M, Szemraj J, Celichowski G, Grobelny J, Krzyzowska M (2018) Tannic acid-modified silver nanoparticles for wound healing: the importance of size. Int J Nanomed 13:991–1007

Pandita D, Munjal A, Poonia N, Awasthi R, Kalonia H, Lather V (2021) Albumin-coated mesoporous silica nanoparticles of docetaxel: preparation, characterization, and pharmacokinetic evaluation. Assay Drug Dev Technol 19(4):226–236

Peng X, Yang G, Shi Y, Zhou Y, Zhang M, Li S (2020) Box-Behnken design based statistical modeling for the extraction and physicochemical properties of pectin from sunflower heads and the comparison with commercial low-methoxyl pectin. Sci Rep 10:1–10

Poltavets YI, Zhirnik AS, Zavarzina VV, Semochkina YP, Shuvatova VG, Krasheninnikova AA, Aleshin SV, Dronov DO, Vorontsov EA, Balabanyan VY, Posypanova GA (2019) In vitro anticancer activity of folate-modified docetaxel-loaded PLGA nanoparticles against drug-sensitive and multidrug-resistant cancer cells. Cancer Nanotechnol 10(1):1–17

Rarokar NR, Khedekar PB (2017) Formulation and evaluation of docetaxel trihydrate loaded self-assembled nanocarriers for treatment of HER2 positive breast cancer. J Drug Deliv Ther 7(6):1–6

Sabio RM, Meneguin AB, Ribeiro TC, Silva RR, Chorilli M (2019) New insights towards mesoporous silica nanoparticles as a technological platform for chemotherapeutic drugs delivery. Int J Pharm 564:379–409

Samanta P, Desai AV, Let S, Ghosh SK (2019) Advanced porous materials for sensing, capture and detoxification of organic pollutants toward water remediation. ACS Sustain Chem Eng 7(8):7456–7478

Sargazi S, Laraib U, Barani M, Rahdar A, Fatima I, Bilal M, Pandey S, Sharma RK, Kyzas GZ (2022) Recent trends in the mesoporous silica nanoparticles with rode-like morphology for cancer theranostics: a review. J Mol Struct 1261:132922

Sawyer S (2009) Analysis of variance: the fundamental concepts. J Manual Manipulat Ther 17(2):27–38

Shelake S, Patil SV, Patil SS, Sangave P (2018) formulation and evaluation of fenofibrate-loaded nanoparticles by precipitation method. Ind J Pharm Sci 80(3):420–427

Sun S, Li B, Yang T, Ma M, Lin Q, Zhao J, Luo F (2018) Preparation and evaluation of smart nanocarrier systems for drug delivery using magnetic nanoparticle and avidin-iminobiotin system. J Nanomater 1:12

Tazeze H, Mequanente S, Nigussie D, Legesse B, Makonnen E, Mengie T (2021) Investigation of wound healing and anti-inflammatory activities of leaf gel of *Aloe trigonantha* L.C. Leach in rats. J Inflamm Res 14:5567–5580

Thambiraj S, Shruthi S, Vijayalakshmi R, Shankaran DR (2019) Evaluation of cytotoxic activity of docetaxel loaded gold nanoparticles for lung cancer drug delivery. Cancer Treat Res Commun 21:100157

Verma A, Dubey J, Verma N, Nayak AK (2017) Chitosan-hydroxypropyl methylcellulose matrices as carriers for hydrodynamically balanced capsules of moxifloxacin HCl. Curr Drug Deliv 14(1):83–90

Wang Z, Zhang N, Chen C, He R, Ju X (2020) Rapeseed protein nanogels as novel pickering stabilizers for oil-in-water emulsions. J Agric Food Chem 68(11):3607–3614
Zhuang J, Li M, Pu Y, Ragauskas AJ, Yoo CG (2020) Observation of potential contaminants in processed biomass using Fourier transform infrared spectroscopy. Appl Sci 10:4345

Publisher's Note